Small Animal ^{13}C-Hyperpolarized MRI: Hardware, Agents & Applications

Authors: M Mattingly, J Kempf, S Madi, E Frederick, T Sasser

Authors Affiliation: Bruker BioSpin, Preclinical Imaging Division, Billerica, MA USA

Hyperpolarization refers to a process of generating molecules with a large, non-equilibrium increase in alignment of nuclear spins with a magnetic field, yielding correspondingly large sensitivity gains for MRI or NMR. ^{13}C-Hyperpolarized (HP) molecules provide a unique signature for molecular processes relevant to a range of disease processes that can be imaged by MRI and promises improved detections for certain indications relative to traditional clinical molecular imaging methods. Preclinical ^{13}C-HP MRI studies have been key in efforts to develop and validate methods and agents for clinical imaging applications. Polarization of agents has been performed using dynamic nuclear polarization (DNP) and parahydrogen induced polarization (PHIP) methods, and imaging has been performed using both dedicated preclinical scanners at fields up to 14 Tesla (T) or clinical scanners. Polarization techniques differ in the range of probes that can be produced and the performance of the resulting product for imaging. Additionally, in part because the lifetime of a hyperpolarized probe is shortened relative to the field of the scanner used, there is a growing trend for preclinical laboratories focused in ^{13}C-H MRI studies to employ relatively small and low field magnets like the Bruker BioSpec 3T, a compact preclinical imaging system that has no need for liquid cryogen filling. In case of the BioSpec 3T, the translational field strength of 3 Tesla further fosters possible translations to clinical 3 Tesla systems and offers the advantage of much stronger gradients to accelerate the image readout. An overview of current and emerging preclinical scanner technology, polarization technologies, and biological applications relevant to ^{13}C-HP-MRI is provided here.

Preclinical ^{13}C-Hyperpolarized MRI: Hardware and Methods

Preclinical MR Scanners, Polarizers, and Workflow

Because ^{13}C-HP agents have a lifetime in the range of only seconds, polarization and scanning hardware typically reside within close-proximity in most laboratories (Kiessling et al., 2017). In fact, researchers will optimize the layout of the laboratory for efficient delivery of the probe from the polarizer to the animal which is pre-positioned within a scanner for immediate imaging (Figure 1).

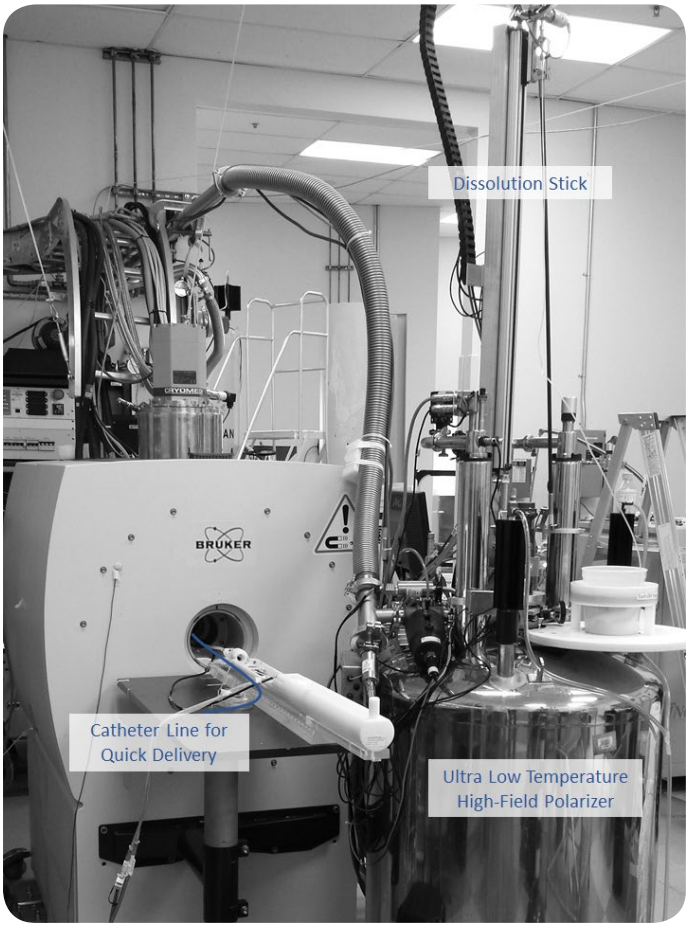

Figure 1. Instrumentation and layout of a typical laboratory conducting small animal ^{13}C-hyperporized studies using the Bruker BioSpec 3T MR system with polarizer positioned adjacent to the scanner. Study animals are positioned in the scanner with a catheter in place for ^{13}C-HP probe delivery for immediate imaging. The DNP polarizer shown includes a compact solid-state microwave (<400 mW) source mounted out of view. The dissolution stick for DNP injection via pneumatic vertical action requires some overhead clearance. Courtesy: Dr. Renuka Sriram, Dr. Sukumar Subramaniam, Dr. Kurhanewicz et al., Pre-Clinical MR Imaging Core, University of California, San Francisco, USA.

Polarizers: DNP

DNP is the most widely used and versatile hyperpolarization method to date (Kiessling et al., 2017). DNP is most effective when applied to solid-state samples frozen at low-temperature. For example, DNP near 100 K typically provides 25-300 fold enhancements in widely used products for solid-state magic-angle spinning (MAS) NMR, enabling previously inaccessible applications ranging from biomolecular structure determination, to drug discovery and materials science. Bruker MAS DNP systems in these fields have been installed in over 30 sites worldwide. Still more dramatic gains >10,000-fold are available for solution-state MRI and NMR using dissolution DNP (d DNP). There, DNP is applied to a frozen solid near just 1 K, then followed by rapid dissolution of the sample by injection of a superheated solvent that both dissolves the sample and pushes it from the cryogenic environment. Despite these impressive conditions for polarization, dissolution and extraction, the result is a sample near room or body temperature with record-setting hyperpolarization levels. This enables a wide range of applications in MRI, particularly in imaging of ^{13}C-labeled metabolites to assess cancer, cardiac function, brain chemistry and more in rapidly expanding array of studies.

There may be room for further improvement in available DNP technologies. As part of an internal preclinical research project conducted by Bruker, a d-DNP polarizer was constructed that operated near 1.1 K and 7T, an optimum range of polarizing conditions yielding as much as 50-70% ^{13}C polarization for various metabolic agents. In addition, the polarizer incorporated high-throughput polarization technique of frequency swept, microwave-gated ^{1}H, ^{13}C cross polarization (CP), capable of >10X reduction of build-up times for ^{13}C polarization without sacrifice to polarization levels. The system accommodated polarization of 20–250 uL samples, convenient for dissolution to volume and dosing for preclinical applications.

Polarizers: PHIP

PHIP polarization has also been employed. PHIP (parahydrogen induced polarization), which has had a long-standing level of scientific activity/development, involves the use of parahydrogen (p H2), which is a hydrogen molecule trapped in a given spin energy state, and therefore hyperpolarized. Currently known methods are categorized as PHIP (parahydrogen induced polarization) or NH-PHIP (non-hydrogenative PHIP). PHIP is a general term used to reference specific approaches in the PASADENA (Bowers et al., 1987) family of experiments (parahydrogen and synthesis allow dramatically enhanced nuclear polarization). The key to that weighty acronym is the word synthesis, referring to the fact that the molecule one wishes to hyperpolarize must be parahydrogenated.

Variations of PHIP have been used to hyperpolarize metabolically interesting species such as pyruvate (Reineri et al., 2015). PHIP is suitable for a smaller range of molecules, those starting with unsaturated bonds. The PHIP reaction typically requires a catalytic co-reagent which often exhibit toxic biological effects. In contrast, NH-PHIP avoids hydrogenation altogether, but still relies on chemical steps to transfer hyperpolarization from p H2 to the molecule of interest. This approach is best known as SABRE (signal amplification by reversible exchange) (Adams et al., 2009) and utilizes the chemically specific step of ligand binding, to bring p H2 and the target molecule together in a catalytic complex. Only molecules containing a convenient lone pair of electrons for donation to the metal catalyst can receive hyperpolarization from a co-bound p H2 molecule. Sensitivity to the on/off kinetics of ligand exchange can limit efficacy. More recent developments promise a broader array of targets by relaying

the hyperpolarization through exchangeable protons in the solvent or a co-solute. PHIP produces lower concentrations and yield polarization levels about 100 times lower than from d-DNP (Lali et al., 2018). Interestingly, Schmidt et al. (2017) recently reported on a liquid-state ^{13}C hyperpolarization protocol performed inside a Bruker BioSpec 7T scanner (obviating the need for a fully dedicated polarizer) allowing for rapid delivery and imaging of some ^{13}C-HP agents.

Preclinical MR Scanners and Hyperpolarized Imaging

A range of MRI technologies have been used in small animal ^{13}C-HP studies. As mentioned above, ^{13}C-HP can be detected even at low fields (Figure 2). In fact, one of the best characterized probes, ^{13}C-pyruvate, has a lifetime approximately 1.5 X longer at 3T versus 14T (Adamson et al., 2017, Chaumeil et al., 2015). Still, numerous studies have been reported in Bruker BioSpec 4.7T, 7.0T, and 9.4T systems (Steinhauser et al., 2018, Oh-Ici et al., 2016, Leftin et al., 2013). MR technologies have relative tradeoffs for laboratories involved in ^{13}C-HP studies, considering cost of ownership and the range of alternative intended uses for the equipment (Table 1). Translational field systems provide suitable performance for HP imaging studies typically at a lower cost of ownership. The BioSpec 3T system is a compact preclinical MR system with no liquid Helium filling that is ideal for ^{13}C-HP applications by offering faster high-resolution image readouts compared to clinical scanners and still allows for a range of alternative preclinical applications. Still, at higher fields (7T and higher), chemically shifted NMR signals will be stronger (for example, separation between the pyruvate and lactate will be 4X greater at 11.7T versus 3T), and this could allow for clearer distinction of ^{13}C-HP probe metabolites of either a single probe or when imaging multiple probes simultaneously. In addition to these general considerations for scanners and ^{13}C-HP MR, there are specific operating and scanning protocol considerations for the time-sensitive imaging required with ^{13}C-HP molecules (Table 2).

Preclinical ^{13}C-HP MRI currently has some limitations in throughput potential which especially limits applications for ^{13}C-HP MRI for basic biological applications where animals are typically imaged longitudinally and in cohorts. This limitation is in part related to the time required to prepare polarized probes. For some polarization systems and reactions, it is possible to produce sufficient probe for multiple animals in a single reaction, however because of the short lifetimes of ^{13}C-HP-agents it is not possible to perform successive scanning to use full- volume available, leaving material to waste. Ramirez et al. (2015) reported on a multi-animal imaging strategy for ^{13}C-HP MRI in a 7 Tesla BioSpec that may allow users to use the full probe produced during a single polarization reaction. Solutions such as this may allow for higher throughput imaging, mitigating some current limitations especially in dedicated biological applications.

Table 1: Bruker BioSpec MR Systems for ^{13}C-HP-MRI

Translational Field MRI	**High-Field MRI**
Bruker BioSpec 3T	**BioSpec, PharmaScan**
	
Easy translation of results and extended lifetime of ^{13}C-HP molecules	Higher spectral separation of ^{13}C-HP agent metabolites
Complete fast imaging sequence portfolio (e.g. EPI, EPSI, FISP) including Parallel Imaging acceleration (GRAPPA)	Complete fast imaging sequence portfolio (e.g. EPI, EPSI, FISP) including Parallel Imaging acceleration (GRAPPA)
Fast imaging with up to 900 mT/m gradients	Fast imaging with up to 1000 mT/m gradients
Field-map based shimming (1st and 2nd order)	Field-map based shimming (up to 3rd order)
Magnet requires no liquid Helium filling	Robust Ultra-Shielded and Refrigerated (USR) magnet technology that stays on field for at least 10 days during a cooling disruption
	^{13}C CryoProbe available for 4X increase in sensitivity

Table 2: Some Gradient, Coil and Method Considerations for Time-Sensitive ^{13}C-HP MRI.

Gradients, Coils, & Peripheral Materials		Strong gradient amplifiers with fast switching of large gradient amplitudes are needed to overcome the inefficiency of low Gamma nuclei like ^{13}C while using EPI based methods.
		Both ^{1}H and ^{13}C (e.g. broadband channel) are required, given that the ^{1}H channel is normally used to provide the morphological image, and local field shimming capability.
		Depending on the region of interest, some combination of ^{13}C volume coil and local receive coil can be used. A local ^{13}C transmit-receive surface coil can also be used with a ^{1}H volume coil.
		Animal beds/holders and solutions for quick injections.
Methods and Sequences for Fast Decaying Non-Recoverable Spin Population	**Timing**	Sequences must be fast on the order of a few seconds
		Total experiment time must be within about 30-60 seconds before polarization or net magnetization is too low (SNR) to be useful.
		Experiment starts around 20 seconds after injection coordinated with the arrival of ^{13}C-HP agent at a target site and initial production of metabolic by-products if applicable (e.g. ^{13}C-lactate production).
	RF Excitation Efficiency	Excitation of spins should not use up the polarization significantly faster than the T1 relaxation time (else spins revert-back to thermal equilibrium state to fast and signal gain is lost). Varying the flip-angle during the experiment provides a good trade-off for SNR at the finish. Only the last RF pulse can be at 90-degree flip.
		Echo Planar excitation and readout sequences, like EPSI, have the most efficient use of magnetization and signal detection, as they rely on refocusing the spins via the spatial readout field gradient during the acquisition, and so use far less RF pulses.
		CSI requires more RF pulses, and thus imposes a SNR loss owing to the smaller flip angles with EPSI.
	Volume of Interest	Localization is done by some combination of coil geometry (local or volume coil) and gradient encoding. The local RF coil, as in ^{1}H MRI and MRS, can be optimized for SNR and spatial selectivity.
		The SINGLEPULSE method (pulse and collect without gradient spatial encoding) of ^{13}C products at a single optimal point in time after injection from localized coil has highest SNR. However, resolution is sacrificed and determined by the local receive RF coil size geometry.
		EPSI or CSI can provide good spatial distribution of ^{13}C-pyruvate and its metabolite products across the active volume of the ^{13}C coil (either local coil for organ (prostate, liver, brain)) or volume coil for region (head, abdomen), depending upon spatial resolution requirements. This is typically taken at an optimal point in time after injection. These spatial dimensions must be on the order of 8x8 to 16x16 elements relative to tradeoffs for SNR and pixel dimensions.
	Dynamic vs Static	A time-course of products (e.g. ^{13}C-pyruvate products such as labeled lactate) are easily followed if no spatial encoding is used which lengthens experiment time considerably.
		Single pulse, single acquisition repeated every second can easily follow the buildup of probe products within the coil region.
		A single spectroscopic image like EPSI can be performed at the optimal point in time where the labeled metabolites are highest, and a good spatial resolution is possible, though at the expense of time resolution.

Preclinical ^{13}C-Hyperpolarized MRI: Agents and Applications

Probe Viability: Toxicity, T1 & Rate of Metabolism

A range of biomolecules have been evaluated as ^{13}C-HP-MRI probes. Some chemical/biochemical properties of molecules influence the suitability and performance for ^{13}C-HP-MR (Chaumeil et al., 2015). To be useful for ^{13}C-HP MRI, molecules should exhibit low toxicity even at mM concentrations. Further, the biomolecular process to be measured with the compound must occur within the short 3X T1 range (typically between 30-180 seconds) for the molecule. The best ^{13}C-HP MR candidates are typically low molecular weight primarily due to the longer T1s of these molecules. As discussed above, the layout of the laboratory is critical for reducing the delivery time of a HP-probe from the polarizer to the sample for immediate scanning. Methods to increase the rate for the biological delivery of the HP-probe may also be adopted. Reynolds et al. (2017) using a 7 Tesla BioSpec, recently showed that arterial injection of ^{13}C-HP probe provided 4.6X tumor signal compared to intravenous injections. This difference is attributed to the more direct vascular delivery to the target site with an arterial injection. This method may further extend the useable range of HP agents, though primarily for preclinical applications.

Figure 2

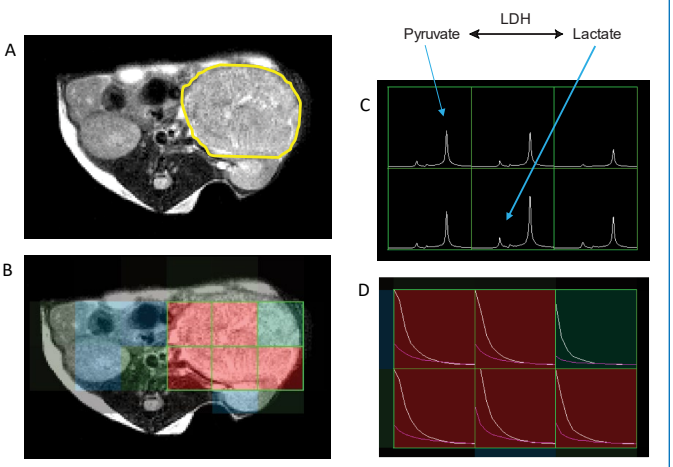

Hyperpolarized ^{13}C metabolic imaging of patient derived renal cell carcinoma orthotopic mouse model. Imaging was performed to investigate metabolic differences in patient derived (PDX) renal cell carcinoma (RCC) models (NIH U01CA217456). Mice were implanted with PDX tissue in the renal capsule and examined using 2D EPSI at 3T (BioSpec 3T) after infusion of hyperpolarized [1-^{13}C] pyruvate. (A) T2 weighted proton image of mouse bearing tumor in the left renal capsule. The yellow dotted line highlights the tumor. (B) Hyperpolarized lactate image overlaid on tumor. (C) Hyperpolarized spectra from each tumor voxel shown in the grid in figure B. (D) Hyperpolarized dynamic traces of pyruvate (yellow) and lactate (pink) from each voxel corresponding to the tumor. Courtesy: Dr. Renuka Sriram, Dr. Sukumar Subramaniam, Dr. Donna Peehl, Dr. Kurhanewicz et al, Pre-Clinical MR Imaging Core, University of California, San Francisco, USA.

Table 3: A Range ^{13}C-Hyperpolarized MR Probes Have Been Evaluated in Preclinical Small Animal Models*

Metabolic Agents	Pyruvate, Acetate, Lactate, Succinate, Glucose, Butyrate, Isocaproate
Perfusion Agents	Urea, HMCP, t-butanol
pH Agents	Bicarbonate, Zymonic Acid
Redox Agents	DHA
Necrosis Agents	Fumarate
Angiography Agents	HEPP
Targeted Agents	TFPP

*For details of chemistries, T1 values, and animal studies, see Brindle et al., 2015, Keshari et al., 2014, Adamson et al., 2017, and the Molecular Imaging and Contrast Agent Database https://www.ncbi.nlm.nih.gov/books/NBK5330/

Probes & Applications Evaluated in Preclinical Studies

^{13}C-pyruvate has become a leading candidate for imaging in large part due to a relatively favorable 3X T1, favorable rate of biological metabolism, and the broad activity of ^{13}C-pyruvate in oncology imaging (Adamson et al., 2017, Brindle et al., 2015, Keshari et al., 2014). The broad utility of 13C-pyruvate MRI and 18FDG/PET for tumor imaging are both attributable at least in part to the tendency for tumor metabolism to shift toward aerobic glycolysis. This metabolic characteristic of tumors is termed the Warburg effect. HP-^{13}C-pyruvate has been employed in MRI preclinical studies of tumor progression and therapeutics (e.g. assessing metabolic changes in a paclitaxel tumor treatment model in a BioSpec 4.7T, Seth et al., 2011) and is currently being assessed in clinical studies. Still, evaluations of new tumor specific probes continue, and performance is often benchmarked to ^{13}C-pyruvate (e.g. assessment of 13C-ethyl acetoacetate in a liver cancer model in a 3T Bruker BioSpec, Jensen et al., 2014).

Both novel and established ^{13}C-HP probes are being assessed in a growing range of disease models (Table 3). Several groups have evaluated a range of non-pyruvate metabolic probes (e.g. ^{13}C-succinate in tumor model in a BioSpec 4.7T, Zacharias et al., 2016), various non-metabolic functional probes (e.g. ^{13}C-Zymonic Acid for measuring tumor pH, Düwel et al., 2017), and perfusion probes (e.g. ^{13}C-Urea for organ perfusion). Of course, the range of proposed ^{13}C-HP-MR applications extends beyond oncology. ^{13}C-hyperpolarized-MRI has been assessed for preclinical cardiology applications (e.g. cardiac ischemia-reperfusion model in a BioSpec 7T, O h-lci et al., 2016), studies of metabolic changes under anesthesia (anesthesia effect on rodent cardiac metabolism in a BioSpec 9.4T, Steinhauser et al., 2018), in rodent models of acute liver disease (e.g. PCA rat model in a BioSpec 7T, Chavarria et al., 2015), and musculoskeletal studies (e.g. exercise stimulation model in a BioSpec 4.7T, Leftin et al., 2013). New applications for ^{13}C-HP-MR are still being revealed. Markovic et al. (2018) recently demonstrated that placental metabolism and perfusion in abnormal pregnancy in rats could be effectively measured using ^{13}C-HP-MR in a BioSpec 4.7T, providing a potentially useful option for diagnostic imaging during abnormal pregnancy and extending the potential applications of ^{13}C-HP-MRI.

Molecular Imaging: ^{13}C-Hyperpolarized MRI & PET

At a general level, MRI is attractive for metabolic imaging because MR can, in principle, provide higher resolution than PET and can be performed without ionizing radiation. Because ^{18}FDG/PET imaging especially has been used most often for both clinical and preclinical metabolic/molecular imaging, some studies have compared the relative performance of ^{13}C-pyruvate-HP MR metabolic imaging versus ^{18}FDG/PET metabolic imaging in disease models. Some critical differences in detections have been noted in some of these studies. For example, ^{13}C-pyruvate HP-MRI performed in a BioSpec 7T system provided an early indicator of therapeutic efficacy in an ovarian tumor therapy model that was not detected by 18FDG/PET (Ravoori et al., 2017). Of further significance, ^{13}C-HP imaging can measure initial reaction rates and enzyme kinetics.

Additionally, ^{13}C-pyruvate can provide more definitive detections for some anatomical regions/conditions. For example, ^{13}C-pyruvate imaging has risen to the forefront in clinical studies of prostate cancer imaging owing in part to the clean signal obtained for imaging at this anatomic region relative to ^{18}FDG/PET which is confounded for this application by non-specific signal from the adjacent bladder where ^{18}FDG clearance occurs. Still, because many molecular processes are outside a reasonable T1 range for hyperpolarized imaging, many molecular detections will still require PET. This will be particularly true for larger compounds such as antibodies (ImmunoPET) that require hours or days (well beyond the lifetime of any polarized probe) for peak uptake and in some cases require long half-life isotopes for the purposes of extending imaging time courses.

Table 4

Insert	**Inline**	
Bruker PET Insert	*Bruker PET Inline*	*Bruker PET/MR 3T*
		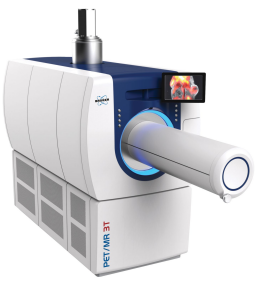
PET ring is mounted inside the magnet bore	PET ring mounted in front of high-field magnet	PET ring mounted in front of magnet
Simultaneous scanning with spatially and temporally registered data	Sequential scanning with spatially registered data	Sequential scanning with spatially registered data
Integrated ParaVision PET/MR workflow	Integrated ParaVision PET/MR workflow	Integrated ParaVision PET/MR workflow
Low attenuation cradles available	Low attenuation cradles available	Low attenuation cradles available
Low attenuation PET coils, with extended FOV designed for optimized simultaneous imaging, are available	Standard bore mounted volume coils can be used	Standard bore mounted volume coils can be used

Some researchers have proposed HyperPET (combined HP-MRI and PET) to capture the full benefits of molecular hyperpolarized MRI and molecular PET (Gutte et al., 2015). This integrated imaging could provide simultaneous detections of multiple metabolic pathways as well as upstream and downstream shifts in metabolism, especially in metabolic imaging (e.g. ^{13}C-HP-pyruvate and its metabolites reside downstream of glucose and the dynamics may vary depending on the metabolic state of the cell) (Gutte et al., 2015). Bruker BioSpec MR systems can now be equipped for multimodal PET/MR (Table 4) that could facilitate the development of novel HyperPET protocols. The Bruker Insert and Inline PET systems have been optimized for integrated imaging, include automated image registration, automated attenuations corrections, and are operated via a single integrated ParaVision interface preloaded with PET/MR scan protocols.

Conclusions

Preclinical hyperpolarized MRI technologies and applications have continued to evolve in the last decade. The Bruker BioSpec 3T MR system without liquid Helium filling is currently installed in multiple labs focused in hyperpolarized imaging and Bruker continues to consider technology advancements to further support this critical application. Bruker's full range of BioSpec MRI systems at up to 15.2T have been used in studies ranging in scope from efforts to develop and test novel polarization technologies, efforts to optimize imaging workflows and methods, and efforts to evaluate agents for applications and indication in oncology, therapeutics, cardiology, and gestation. An emerging area under study will be related to the possible synergies of multimodal functional imaging using ^{13}C-HP MRI and PET.

References

Kiessling F, Pichler BJ, Hauff P. (2017) Small Animal Imaging (Second Edition). Chapter 13 MRI, In Vivo Magnetic Resonance Imaging and Spectroscopy with Hyperpolarized Agents, 286.

Bowers CR, Weitekamp, DP. (1987) Parahydrogen and synthesis allow dramatically enhanced nuclear alignment. J Am Chem Soc. 109:5541–5542.

Reineri F, Boi T, Aime S. (2015) ParaHydrogen Induced Polarization of ^{13}C carboxylate resonance in acetate and pyruvate. Nat Commun. 6:5858.

Adams RW, Aguilar JA, Atkinson KD, Cowley MJ, Elliott PI, Duckett SB, Green GG, Khazal IG, López-Serrano J, Williamson DC. (2009) Reversible interactions with para-hydrogen enhance NMR sensitivity by polarization transfer. Science. 323(5922):1708-11.

Iali W, Rayner PJ, Duckett SB. (2018) Using parahydrogen to hyperpolarize amines, amides, carboxylic acids, alcohols, phosphates, and carbonates. Sci Adv. 5;4(1).

Schmidt AB, Berner S, Schimpf W, Müller C, Lickert T, Schwaderlapp N, Knecht S, Skinner JG, Dost A, Rovedo P, Hennig J, von Elverfeldt D, Hövener JB. (2017) Liquid-state carbon-13 hyperpolarization generated in an MRI system for fast imaging. Nat Commun. 6;8:14535.

Adamson EB, Ludwig KD, Mummy DG, Fain SB. (2017) Magnetic resonance imaging with hyperpolarized agents: methods and applications. Phys Med Biol. 62(13):R81-R123.

Chaumeil MM, Najac C, Ronen SM. (2015) Studies of Metabolism Using ^{13}C MRS of Hyperpolarized Probes. Methods in Enzymology, Volume 561:1-71.

Steinhauser J, Wespi P, Kwiatkowski G, Kozerke S. (2018) Assessing the influence of isoflurane anesthesia on cardiac metabolism using hyperpolarized [13C]pyruvate. NMR in Biomedicine. 31:e3856.

Oh-Ici D, Wespi P, Busch J, Wissmann L, Krajewski M, Weiss K, Sigfridsson A, Messroghli D, Kozerke S. (2016) Hyperpolarized Metabolic MR Imaging of Acute Myocardial Changes and Recovery after Ischemia-Reperfusion in a Small-Animal Model. Radiology. 278(3):742-51.

Leftin A, Degani H, Frydman L. (2013) In vivo magnetic resonance of hyperpolarized [(13)C1]pyruvate: metabolic dynamics instimulated muscle. Am J Physiol Endocrinol Metab. 305(9):E1165-71.

Ramirez MS, Lee J, Walker CM, Chen Y, Kingsley CV, De La Cerda J, Maldonado KL, Lai SY, Bankson JA. (2015) Feasibility of multianimal hyperpolarized (13) C MRS. Magn Reson Med. 73(5):1726-32.

Reynolds S, Metcalf S, Cochrane EJ, Collins RC, Jones S, Paley MNJ, Tozer GM. (2017) Direct arterial injection of hyperpolarized $_{13}$C-labeled substrates into rat tumors for rapid MR detection of metabolism with minimal substrate dilution. Magn Reson Med. 78(6):2116-2126.

Brindle KM. (2015) Imaging metabolism with hyperpolarized (^{13})C-labeled cell substrates. J Am Chem Soc. 137(20):6418-27.

Keshari KR, Wilson DM. (2014) Chemistry and biochemistry of ^{13}C hyperpolarized magnetic resonance using dynamic nuclear-arpolarization. Chem Soc Rev. 7;43(5):1627-59. doi: 10.1039/c3cs60124b.

Seth P, Grant A, Tang J, Vinogradov E, Wang X, Lenkinski R, and Sukhatme VP (2011) On-target Inhibition of Tumor Fermentative Glycolysis as Visualized by Hyperpolarized Pyruvate. Neoplasia. 13(1): 60–71.

Jensen PR, Serra SC, Miragoli L, Karlsson M, Cabella C, Poggi L, Venturi L, Tedoldi F, Lerche MH. (2015) Hyperpolarized [1,3-^{13}C2]ethyl acetoacetate is a novel diagnostic metabolic marker of liver cancer. Int J Cancer. 136(4):E117-26.

Düwel S, Hundshammer C, Gersch M, Feuerecker B, Steiger K, Buck A, Walch A, Haase A, Glaser SJ, Schwaiger M, Schilling F. (2017) Imaging of pH in vivo using hyperpolarized ^{13}C-labelled zymonic acid. Nat Commun. 11;8:15126.

Chavarria L, Romero-Giménez J, Monteagudo E, Lope-Piedrafita S, Cordoba J. (2015) Real-time assessment of ^{13}C metabolism reveals an early lactate increase in the brain of rats with acute liver failure. NMR Biomed. 28(1):17-23.

Markovic S, Fages A, Roussel T, Hadas R, Brandis A, Neeman M, Frydman L. (2018) Placental physiology monitored by hyperpolarized dynamic 13C magnetic resonance. PNAS. 6;115(10):E2429-E2436.

Ravoori MK, Singh SP, Lee J, Bankson JA, Kundra V. (2017) In Vivo Assessment of Ovarian Tumor Response to Tyrosine Kinase Inhibitor Pazopanib by Using Hyperpolarized ^{13}C-Pyruvate MR Spectroscopy and ^{18}F-FDG PET/CT Imaging in a Mouse Model. Radiology. 285(3):830-838.

Gutte H, Hansen AE, Henriksen ST, Johannesen HH, Ardenkjaer-Larsen J, Vignaud A, Hansen AE, Børresen B, Klausen TL, Wittekind AM, Gillings N, Kristensen AT, Clemmensen A, Højgaard L, Kjær A. (2015) Simultaneous hyperpolarized (13)C-pyruvate MRI and (^{18})F-FDG-PET in cancer (hyperPET): feasibility of a new imaging concept using a clinical PET/MRI scanner. Am J Nucl Med Mol Imaging. 15;5(1):38-45.

Bruker BioSpin
www.bruker.com